ECCM21

02-05 July 2024 | **Nantes - France**

Proceedings of the 21st European Conference on Composite Materials

Vol 8

Special Sessions

WWW.ECCM21.ORG

UNDER THE PATRONAGE OF:

ESCM European Society For Composite Materials

Association pour les MAtériaux Composites AMAC

EuCIA The European Voice of Composites

WITH THE SUPPORT OF:

RÉGION PAYS DE LA LOIRE

ORGANIZED BY:

CENTRALE NANTES

Nantes Université

SUPPORTING PARTNER:

JEC CONNECTING THE WORLD WITH COMPOSITES

Edited by:

Prof. Christophe BINETRUY
ECCM21 Conference Chair
Institute of Civil Engineering and Mechanics (GeM)
Centrale Nantes
Nantes Université

Prof. Frédéric JACQUEMIN
ECCM21 Conference Co-Chair
Institute of Civil Engineering and Mechanics (GeM)
Nantes Université

Published by:

The European Society for Composite Materials (ESCM) and the Ecole Centrale de Nantes.

These Proceedings have an ISBN (owned by the Publisher) and a DOI (owned by the Ecole Centrale de Nantes).

ISBN: 978-2-912985-01-9
DOI: 10.60691/yj56-np80

Disclaimer:

Editorial

Each volume gathers contributions on specific topics:

- **Vol 1. Industrial applications**
- **Vol 2. Material science**
- **Vol 3. Material and Structural Behavior – Simulation & Testing**
- **Vol 4. Experimental techniques**
- **Vol 5. Manufacturing**
- **Vol 6. Multifunctional and smart composites**
- **Vol 7. Life cycle performance**
- **Vol 8. Special Sessions**

This collection contains the proceedings of the 21st European Conference on Composite Materials (ECCM21), held in Nantes, France, July 2-5, 2024. ECCM21 is the 21st in a series of conferences organized every two years by the members of the European Society of Composite Materials (ESCM). As some of the papers in this collection show, this conference reaches far beyond the borders of Europe.

The ECCM21 conference was organized by the Nantes Université and the Ecole Centrale de Nantes, with the support of the Research Institute in Civil and Mechanical Engineering (GeM).

Nantes, the birthplace of the novelist Jules Verne, is at the heart of this edition, as are the imagination and vision that accompany the development of composite materials. They are embodied in the work of numerous participants from the academic world, but also of the many industrialists who are making a major contribution to the development of composite materials. Industry is well represented, reflecting the strong presence of composites in many application areas.

With a total of 1,064 oral and poster presentations and over 1,300 participants, the 4-day event enabled fruitful exchanges on all aspects of composites. The topics that traditionally attracted the most contributions were fracture and damage, multiscale modeling, durability, aging, process modeling and simulation and additive manufacturing.

However, the issues of energy and environmental transition, and more generally the sustainability of composite solutions, logically appear in this issue as important contextual elements guiding the work being carried out. This includes bio-sourced composites, material recycling and reuse of parts, the environmental impact of solutions, etc.

We appreciated the high level of research presented at the conference and the quality of the submissions, some of which are included in this collection. We hope that all those interested in the progress of European composites research in 2024 will find in this publication sources of inspiration and answers to their questions.

Prof. Christophe BINETRUY
ECCM21 Conference Chair
Institute of Civil Engineering and Mechanics (GeM)
Centrale Nantes
Nantes Université

Prof. Frédéric JACQUEMIN
ECCM21 Conference Co-Chair
Institute of Civil Engineering and Mechanics (GeM)
Nantes Université

Under the Patronage of:

ESCM European Society For Composite Materials

AMAC Association pour les MAtériaux Composites

EuCIA The European Voice of Composites

Organized by: CENTRALE NANTES | Nantes Université

With the support of: RÉGION PAYS DE LA LOIRE

Supported by: EMC2 | JEC CONNECTING THE WORLD WITH COMPOSITES

Sponsored by:

Bronze Partner: BRUKER | INSTRON | MatchID Metrology beyond colors

---

Other partners: CAPACITÉS De la recherche à l'innovation | CARBON AXIS | CETIM

Depestele | EikoSim | ELSEVIER | FAIRMAT

metravib material testing | NOVITOM | Quantiflex simulations | Surface Measurement Systems World Leader in Sorption Science

Hosting Organizations

Conference chairs

Prof. Christophe BINETRUY
ECCM21 Conference Chair
Institute of Civil Engineering and Mechanics (GeM)
Centrale Nantes
Nantes Université

Prof. Frédéric JACQUEMIN
ECCM21 Conference Co-Chair
Institute of Civil Engineering and Mechanics (GeM)
Nantes Université

International Scientific Committee

Malin Akermo (Sweden)
Remko Akkerman (Netherlands)
Andrey Aniskevich (Latvia)
Leif Asp (Sweden)
Emmanuel Baranger (France)
Janice Barton (UK)
Johnny Beaugrand (France)
Andrea Bernasconi (Italy)
Christophe Binetruy (France)
Thomas Bohlke (Germany)
Alain Bourmaud (France)
Nicolas Boyard (France)
Joël Breard (France)
Richard Butler (UK)
Baris Caglar (Netherlands)
Pedro Camanho (Portugal)
Pierpaolo Carlone (Italy)
Paolo Andrea Carraro (Italy)
Valter Carvelli (Italy)
Nuno Correia (Portugal)
Gergely Czél (Hungary)
Clemens Dransfeld (Netherlands)
Sylvain Drapier (France)
Klaus DRECHSLER (Germany)
Andreas ECHTERMEYER (Norway)
Paolo Ermanni (Switzerland)
Martin Fagerström (Sweden)
Ewald Fauster (Austria)
Julien Ferec (France)
Antonio Ferreira (Portugal)
Bodo Fiedler (Germany)
Stefanos Giannis (UK)
Nathalie Godin (France)
Carlos Gonzalez (Spain)
Sotirios Grammatikos (Norway)
Christoph Greb (Germany)
Emile Greenhalgh (UK)
Gianmarco Griffini (Italy)
Stephen Hallett (UK)
Nahiene Hamila (France)
Roland Hinterhoelzl (Austria)
Martin Hirsekorn (France)
Darko Ivančević (Hungary)
Frédéric Jacquemin (France)
Mikko Kanerva (Finland)
Luise Karger (Germany)
Vassilis Kostopoulos (Greece)
Theodosia Kourkoutsaki (Germany)
Thomas Kruse (Germany)
Ugo Lafont (France)
Jacques Lamon (France)
Frédéric Laurin (France)
Antoine Le Duigou (France)
Stepan Lomov (Belgium)
Theodoros Loutas (Greece)
Staffan Lundstrom (Sweden)
António Marques (Portugal)
David May (Germany)
Véronique Michaud (Switzerland)
Jörg Mussig (Germany)
Thomas Neumeyer (Germany)
Philippe Olivier (France)
Alkiviadis Paipetis (Greece)
Federico Paris (Spain)
Chung Hae Park (France)
John-Alan Pascoe (Netherlands)
Alessandro Pegoretti (Italy)
Ton Peijs (UK)
Rob Pierce (Denmark)
Soraia Pimenta (UK)
Silvestre Pinho (UK)
Gerald Pinter (Austria)
Connie Qian (UK)
Marino Quaresimin (Italy)
Andrew Rhead (UK)
Paul Robinson (UK)
Essi Sarlin (Finland)
Yentl Swolfs (Belgium)
Sofia Teixeira du Freitas (Netherlands)
Julie Teuwen (Netherlands)
Ole Thomsen (UK)
Stavros Tsantzalis (Greece)
Konstantinos Tserpes (Greece)
Albert Turon (Spain)
Julien van Campen (Netherlands)
Wim Van Paepegem (Belgium)
Anastasios Vassilopoulos (Switzerland)
Ignaas Verpoest (Belgium)
Michael Wisnom (UK)
Dimitrios Zarouchas (Netherlands)
Daiva Zeleniakiene (Lithuania)
Dan Zenkert (Sweden)

Local Organizing Committee

Suresh Advani
Romain Agogué
Sylvain Chataigner
Sébastien Comas-Cardona
Sofiane Guessasma
Suzanne Laïk
Philippe Le Bot
Mael Peron
Luisa Silva
Vincent Sobodka
Alexandre Ripoche
Elena Syerko

x

CONTENTS

Table of Contents

THE EFFECTS OF STACKING SEQUENCE ON COMPOSITE COMPRESSIVE PERFORMANCE AND HOW TO IMPROVE IT

Joe Rifai[1], Xun Wu[2], Laura Rhian Pickard[3], Giuliano Allegri[4], and Michael R. Wisnom[5]

[1,2,3,4,5]Bristol Composites Institute, Civil, Aerospace, and Design Engineering Department, University of Bristol, Queen's Building, BS8 1TR, Bristol, United Kingdom.
[1]Email: Joe.rifai@bristol.ac.uk,
[2]Email: Xunxun.wu@bristol.ac.uk,
[3]Email: Laura.pickard@bristol.ac.uk,
[3]Web Page: https://research-information.bris.ac.uk/en/persons/laura-rhian-pickard
[4]Email: Giuliano.allegri@bristol.ac.uk,
[4]Web Page: https://research-information.bris.ac.uk/en/persons/giuliano-allegri
[5]Email: M.Wisnom@bristol.ac.uk,
[5]Web Page: https://research-information.bris.ac.uk/en/persons/michael-r-wisnom

Keywords: Sandwich structure, Stacking sequence, Compression, Four-point bend test

Abstract

Uni-directional fibre-reinforced composites demonstrate a lack of mechanical strength in compression Experimental tests according to ASTM D5467 were used to obtain the compressive performance of IM7/8552 unidirectional carbon fibre with various stacking sequences. The response shows a reduction in stiffness with increasing strain. An analysis of the non-linear stiffness of the different configurations shows that the non-linear stiffness variation is similar for uni-directional and multi-directional laminates. Experimental results show that the initial stiffnesses of multi-directional laminates are similar to those calculated using classical laminate plate theory. The uni-directional laminate shows a longitudinal stiffness of 15% less than expected. Uni-directional, cross-ply, and quasi-isotropic laminates show a non-linear longitudinal stiffness reduction of 7% at an applied compressive strain of 1%.

1. Introduction

The effects of the stacking sequence on composites remain an area of interest for composite engineers to identify the optimum positioning of higher stiffness plies. Fibre-reinforced composites demonstrate higher mechanical properties in tension failure rather than compression failure. Tensile loading of composites can support the alignment of the reinforcement fibres [1]. However, composites loaded in compression may cause the fibre reinforcement to buckle leading to a kink-band failure [2]. This failure occurs due to shear instability and micro-buckling of fibres caused by fibre waviness and voids [3, 4].

The stacking sequence affects the bending stiffness matrix. Minimal consideration has been given to the effect of stacking sequence on strength due to challenges with testing, although bending stiffness has a significant influence on buckling performance [5, 6]. An in-situ compressive test with a scanning electron microscope was used to observe the failure process at the microscale of composites in compression [7]. Failure initiation occurs through shear instability of the fibre and is caused by compressive stresses that cause small fibre rotations and fibre misalignment. The purpose of this study is to review the stacking sequence and positioning of highly loaded fibre reinforcement to relate the compressive strengths of multi-directional laminates to fundamental unidirectional material strengths.

2. Specimen Design and Preparation

The design of the sandwich structure was based on ASTM D5467 standard [8, 9]. Acrylic PMMA, poly (methyl methacrylate), was selected as the core material due to a high shear strength of 62 MPa, and a stiffness of 2.96 GPa. The effects of the strain gradient on failure strain were considered, to identify suitable beam thickness, and results show no significant constraint effect if the beam thickness is above 14 mm [8]. Sample dimensions were modified to reduce high applied loads, eliminate core shear failure, and allow for specimen machinability. The structure length was 650 mm and consisted of top and bottom laminates each manufactured from eight plies of uni-directional IM7-8552 to obtain 1 mm thick laminates and an acrylic PMMA core of 15 mm thickness. The composite material properties for IM7-8552 Hexply® were obtained according to the manufacturer's datasheet [10] and experimental findings [4, 11, 12]. The inputs used were $E_{11} = 161\ GPa$, $E_{22} = 11.4\ GPa$, $G_{12} = 5.17\ GPa$, and $\nu_{12} = 0.32$. IM7-8552 material properties were used in classical laminate plate theory (CLPT) to calculate the laminate stiffness shown in Table 1.

Table 1. Laminate properties for uni-directional, quasi-isotropic, and cross-ply laminates.

Laminate configuration	Longitudinal Stiffness (GPa)	Transverse Stiffness (GPa)	Poisson's ratio
Uni − directional	161	11.4	0.32
Quasi − isotropic	61.7	61.7	0.32
Cross − ply	86.7	86.7	0.05

Two arrangements were specified for the top laminate to investigate the objectives of determining the influence of stacking sequence and positioning of highly loaded fibres. Arrangement one is a quasi-isotropic with different stacking sequences $[0/90/\pm 45]_s$, $[\pm 45/90/0]_s$, and $[+45/0/-45/90]_s$. Arrangement two is a cross-ply that consists of $[0_2/90_2]_s$ and $[90_2/0_2]_s$. The neutral axis ($\bar{y}$) was calculated based on Equation 1. The area (A) and component centroid (y) were calculated based on the sample dimensions provided in Figure 1, considering the stiffness contribution of each component. The stiffness contribution factor of the top skin (E_t), core (E_c), and bottom skin (E_b) are shown in Table 1.

$$\bar{y} = \frac{\sum\left(\frac{E_t}{E_C} * b_t * d_t * y_t\right) + (b_c * d_c * y_c) + (\frac{E_b}{E_C} * b_b * d_b * y_b)}{\sum\left(\frac{E_t}{E_C} * b_t * d_t\right) + (b_c * d_c) + (\frac{E_b}{E_C} * b_b * d_b)} \tag{1}$$

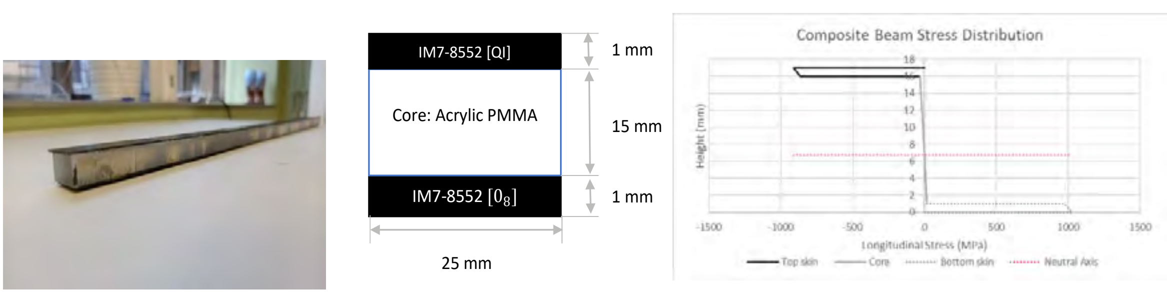

Figure 1. Composite sandwich structure (left), cross-section view of composite sandwich structure (middle), and composite beam stress distribution showing neutral axis for cross-ply sample (right).

Table 2. Top laminate configuration showing stiffness and distance of the neutral axis of the structure.

Top laminate	Quasi-isotropic	Cross-ply
Longitudinal Compressive Stiffness (GPa)	61.7	86.7
Distance of neutral axis (mm)	5.87	6.52

IM7-8552 laminates were manufactured and cured in the autoclave using the manufacturer's cure cycle [10]. The PMMA core material was treated using a grit blaster to provide a rough surface for bonding. The top and bottom laminates were sanded using P100 grit paper. Araldite® 2021-1 paste epoxy adhesive that cures at room temperature was used to bond the core and skins together with an applied pressure to achieve a bond line thickness of 0.2 mm on each skin. A second batch of materials was bonded using Araldite® 2022-1 paste epoxy adhesive due to better adhesion performance. The sample weight averaged 35.5 ± 0.5 grams with measurements provided in Table 3. Vishay Precision strain gauge (C4A-06-125SL-35039P) was positioned and bonded to the centre of the specimen's top layer to obtain longitudinal and transverse strain measurements.

Table 3. Sample dimensions post bonding.

Configuration	$[0_2/90_2]_s$	$[90_2/0_2]_s$	$[0/90/\pm45]_s$	$[\pm45/90/0]_s$	$[+45/0/-45/90]_s$
$Thickness\ (mm)$	17.53	17.42	17.42	17.32	17.31
$Tolerance\ (mm)$	±0.11	±0.19	±0.19	±0.15	±0.15

3. Experimental Setup and Equipment

The compressive performance of composite reinforced fibres is difficult to measure and shows high variability of test results. The development of compressive test methods is essential to obtain correct failure and true compressive stress results [13]. Most compressive tests of composites show modified fixtures and testing techniques to try to avoid premature failure. Composites show signs of premature failure when tested in compression due to edge failure and localized failure due to stress concentrations. ASTM D6641 standard is a direct compression test in which samples may experience edge delamination [14]. Localised failure is caused by specimen grips that create through-thickness stresses. The ASTM D5467 standard aims at identifying compressive properties of unidirectional polymer matrix composites using sandwich beam arrangements. The test applies a compressive load on the upper skin using a four-point flexural loading system [9].

Flexural tests use load fixtures that require wide rollers with large diameters and loading pads to avoid localized failure of the sandwich beams [8]. Suggestions of the sample dimensions are provided to conduct tests adhering to ASTM D5467 standards [9]. The ASTM standard dimensions have been modified to increase sample length and generate higher compressive stresses while reducing shear stresses on the structure [10]. The shear stresses generated can cause shear failure in the composite sandwich core causing separation of the skin and core.

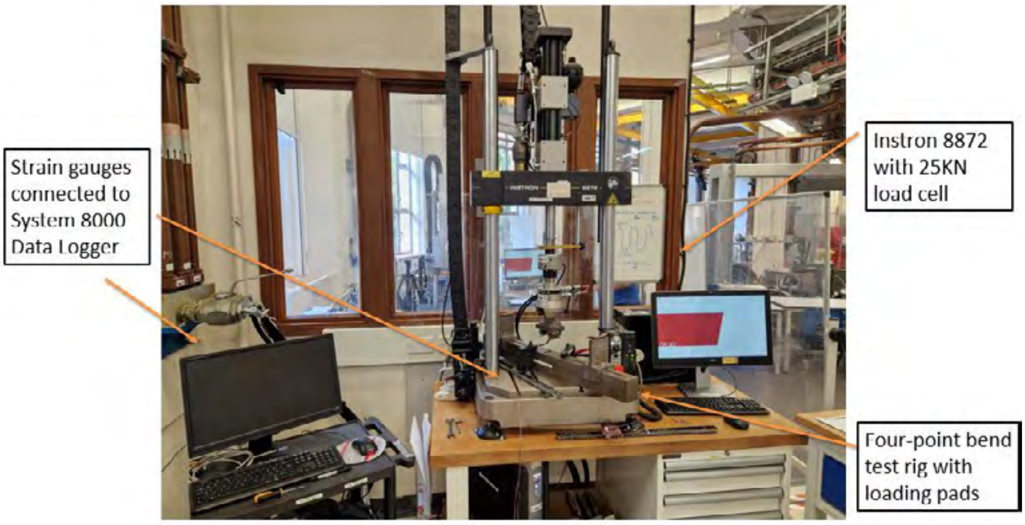

Figure 2. Experimental set-up for compression test of sandwich specimens.

The flexural test required the use of a four-point bend test fixture that is placed on the sample's mid-span length. The mid-span region will experience the highest applied moment where the specimen's compressive performance can be measured. Strain gauges are positioned on the top laminate to measure surface strains. A data logger records the strain measurements with the applied load to identify the stress applied to the laminate.

4. Experimental Results and Discussion

Six samples of each of the following quasi-isotropic laminates ($[0/90/\pm45]_s$, $[\pm45/90/0]_s$, and $[+45/0/-45/90]_s$) were tested. Failure in the gauge section of the top laminate was achieved in some cases. The material's expected compressive failure strain is 1.1% [10]. The maximum compressive failure strains were not achieved due to the debonding between the top skin and the core. However, stiffness results were provided to review the effects of the stacking sequence on composites under compression. Table 4 shows the laminate stiffness calculated from experimental data is similar to that of Table 1. Force and strain results were outputted from the Instron 8872 test machine and System 8000 data logger. The applied bending moment was calculated based on the force (F) at the applied roller distance (L). The flexural strength of the top skin of the beam was determined using an equation derived from simple beam theory [8]. The maximum bending moment at the gauge section was used to calculate the compressive stress on the top skin based (σ_t) in Equation 2.

$$\sigma_t = \frac{\frac{FL}{2} * (y_t - \bar{y})}{I} * \frac{E_t}{E_c} \tag{2}$$

The distance away from the neutral axis ($\bar{y}$) is presented in Table 2, and the top skin height (y_t) is presented in Table 3. The second moment of area (I) was calculated using an equivalent value weighted by the moduli that varies depending on the stiffness contribution of the top skin, core, and bottom skin. The stiffness contribution factor of the top skin (E_t), and core (E_c) must be considered to calculate the compressive stress applied to the top skin. Experimental results in Figure 3 show that the $[0/90/\pm45]_s$ laminate demonstrates a marginal increase in stiffness; however, these results aren't statistically significant to conclude that the position of highly loaded fibres (0-degree ply) further away from a laminate's plane of symmetry increases the laminates' stiffness.

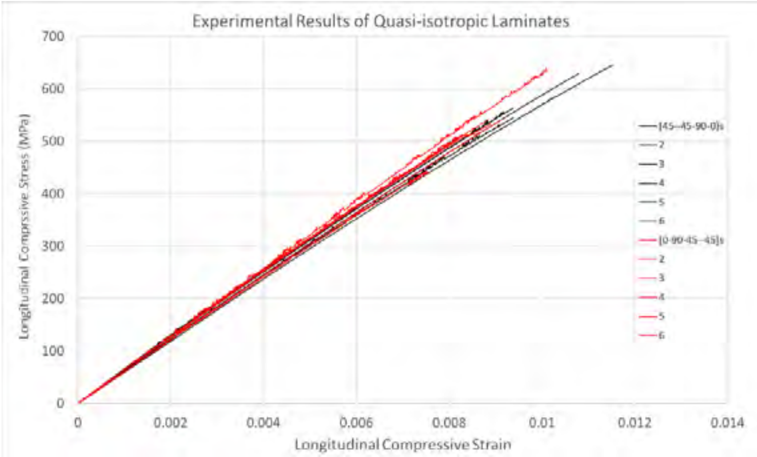

Figure 3. Experimental results of quasi-isotropic laminates showing two different stacking sequences.

Table 4. Compressive stress and stiffness of quasi-isotropic laminates at 0.9% compression strain.

Configuration	$[\pm 45/90/0]_s$		$[+45/0/-45/90]_s$		$[0/90/\pm 45]_s$	
	Compressive Stress (MPa)	Stiffness (GPa)	Compressive Stress (MPa)	Stiffness (GPa)	Compressive Stress (MPa)	Stiffness (GPa)
Sample 1			519.5	57.7		
Sample 2	516.9	57.4	528.8	58.7	546.0	60.7
Sample 3	517.8	57.5	541.1	60.1	533.1	59.2
Sample 6	496.9	55.1	495.5	55.0	523.9	58.2
Average	510.5	56.7	521.2	57.9	534.4	59.3
Standard deviation	11.7	1.3	19.2	2.1	11.0	1.2

Seven samples of each of the following arrangements of the cross-ply laminates ($[0_2/90_2]_s$ and $[90_2/0_2]_s$) were tested. Figure 4 shows the results of the cross-ply laminates, indicating that the $[90_2/0_2]_s$ laminate has a marginal increase in the laminate's compressive stiffness, although the result is not statistically significant. Table 5 shows that the average compressive stress and stiffness of the $[90_2/0_2]_s$ laminate is marginally higher.

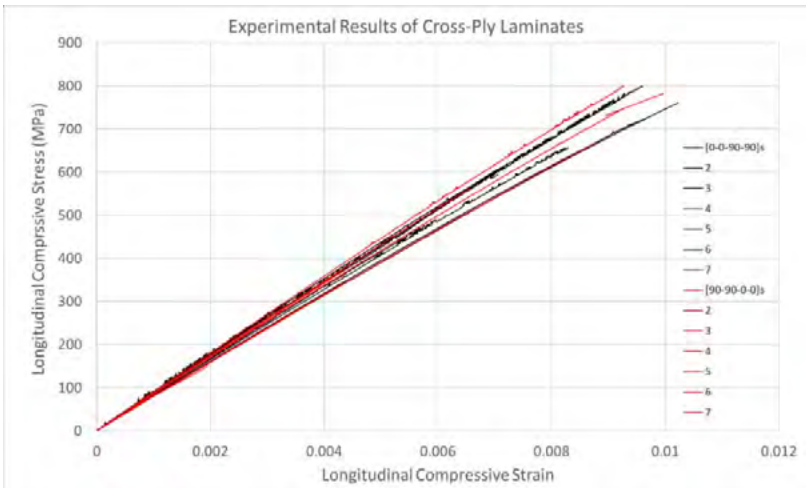

Figure 4. Experimental results of cross-ply laminates showing two different stacking sequences.

Table 5. Compressive stress and stiffness of cross-ply laminates at 0.9% compression strain.

Configuration	$[0_2/90_2]_s$		$[90_2/0_2]_s$	
	Compressive Stress (MPa)	Stiffness (GPa)	Compressive Stress (MPa)	Stiffness (GPa)
Sample 2	785.0	87.1		
Sample 4			823.0	91.4
Sample 6	724.2	80.4	713.3	79.2
Sample 7	722.3	80.2	772.7	85.9
Average	743.8	82.6	769.7	85.4
Standard deviation	35.7	3.9	54.9	5.6

The results for the multidirectional laminates show stiffnesses similar to those calculated using CLPT as seen from the comparison of the dashed and solid lines at zero strain in Figure 5. Further tests were conducted on a unidirectional $[0_4]$ laminate resulting in lower longitudinal stiffness than specified in the data sheet. Composite materials have a non-linear stiffness as further compressive strains are applied. Figure 5 shows a reduction of laminate stiffness as higher compressive strains are applied to composites. A reduction of laminates' longitudinal stiffness is observed showing the non-linearity of composite materials.

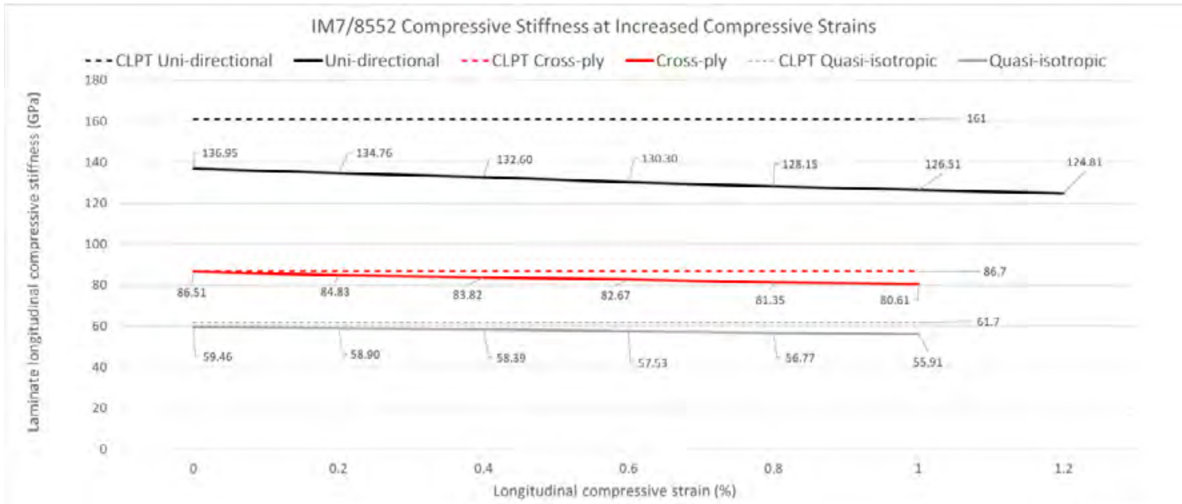

Figure 5. Longitudinal stiffness of quasi-isotropic, cross-ply, and unidirectional laminates at higher compressive strains.

Experimental results in Figure 5 show the longitudinal stiffness for uni-directional, cross-ply, and quasi-isotropic laminates at different compressive strains. All laminate configurations show the same experimental non-linear stiffness reduction of nearly 7% in longitudinal stiffness from the initial measurements up to 1% compressive strain. However, uni-directional laminates show a lower longitudinal stiffness than that in the datasheet. The latter modulus of 161 GPa in comparison to initial readings of 136.95 GPa, a 15% reduction in the expected longitudinal stiffness. The use of multi-directional laminates provides closer laminate stiffness predictions to those calculated using CLPT.

5. Conclusion

Compressive tests of composite materials are challenging due to experimental complexities that can cause stress concentrations or unexpected material failure thus the difficulty in obtaining the compressive strength. A range of stacking sequences were used for the quasi-isotropic and cross-ply laminates. The effects of the stacking sequence show a negligible improvement in laminate stiffness.

The design of composite laminates under compression must be considered as the material shows non-linearity as further compressive strains are applied. Results shown in Figure 5 show a similar reduction of stiffness as further compressive strains are applied for all different laminate configurations. Multi-directional laminates show closer stiffness prediction to CLPT than that of unidirectional laminates. The non-linear stiffness variation for uni-directional, cross-ply, and quasi-isotropic laminates show a similar reduction of 7% in longitudinal compressive stiffness at an applied compressive strain of 1%.

Acknowledgements

The author acknowledges funding for this research provided by the UK Engineering and Physical Sciences Research Council (EPSRC) Programme Grant EP/T011653/1, Next Generation Fibre-Reinforced Composites (NextCOMP): A Full-Scale Redesign for Compression in collaboration with the Imperial College London, and Centre for Doctoral Training in Composites Science, Engineering, and Manufacturing at Bristol Composites Institute in the University of Bristol. For the purpose of open access, the authors have applied a creative commons attribution (CC BY-NC 4.0) license to any author accepted manuscript version arising.

References

[1] B. Wang, G. Fang, X. Tan, J. Liang, J. Ge, & S. Liu. Investigation on the longitudinal compressive strength of unidirectional carbon fiber/nanoparticles reinforced polymer composites using FFT-based method. *Composite Structures*, Vol. (247), 2020. Available from: https://doi.org/10.1016/j.compstruct.2020.112448

[2] J. Bai. *Advanced Fiber-Reinforced Polymer (FRP) Composites for Structural Applications (Second Edition)*. Woodhead Publishing Series in Civil and Structural Engineering, Woodhead Publishing. 2023. Available from: https://doi.org/10.1016/B978-0-12-820346-0.09990-1

[3] B. W. Rosen. Mechanics of composite strengthening. "Fibre Composite Materials." *American Society of Metals.* Chapter 3, P. 37-75, 1965.

[4] S. May & S. Hallett. A Combined Model for Initiation and Propagation of Damage under Fatigue Loading for Cohesive Interface Elements. *Composites Part A – Applied Science*, P.1787-1796, 2010.

[5] K. Schneider. Determination of compressive properties of fibre composites in the in-plane direction according to ISO 14126. Part 1: A round Robin test. *Applied Composite Materials.* Vol. (14), Pages: 1–15, 2007. Available from: https://doi.org/10.1007/s10443-006-9027-6

[6] C.B. York. New Insights into Stiffness Matching between Standard and Double Angle-ply Laminates. *Asian-Australian Conference on Composite Materials*, Cairns, Australia. 2018.

[7] C.V. Opelt, G.M. Cândido, & M.C. Rezende. Compressive failure of fibre reinforced polymer composites – A fractographic study of the compression failure modes. *Materials Today Communications*, Vol. (15), P. 218-227, 2018. Available from: https://doi.org/10.1016/j.mtcomm.2018.03.012

[8] X. Wu, & M.R. Wisnom. Compressive Failure Strain of Unidirectional Carbon Fibre Composites from Bending Tests. *Composite Structures,* Vol. (304), Pages: 1164-1167, 2022. Available from: https://doi.org/10.1016/j.compstruct.2022.116467

[9] ASTM Standard D5467. *"Compressive Properties of Unidirectional Polymer Matrix Composites,"* ASTM International, West Conshohocken, PA, 2017.

[10] Hexcel. HexPly-8552 Datasheet [Online]. Available from: HexPly_8552_eu_DataSheet(1).pdf (hexcel.com)

[11] W. Jiang, S. Hallett, B. Green, & M.R. Wisnom. A concise Interface Constitutive law for Analysis of Delamination and Splitting in Composite Materials and its Application to Scaled Notched Tensile Specimens. *International Journal for Numerical Methods in Engineering*, P. 1982-1995, 2007.

[12] P. Camanho, P. Maimi, & C. Davila. Prediction of Size Effects in Notched Laminates using Continuum Damage Mechanics. *Composite Science and Technology Journal*, P. 2715-2727, 2007.

[13] P. Berbinau, C. Soutis, & I.A. Guz. Compressive failure of 0° unidirectional carbon-fibre reinforced plastic (CFRP) laminates by fibre micro buckling. *Composite Science Technology*. Vol. (59), P.1451–1455, 1999. Available from: https://doi.org/10.1016/S0266-3538(98)00181-X

[14] ASTM Standard D6641. *Compressive Properties (CLC)*. ASTM International, West Conshohocken, PA, 2023.

ECCM21

02-05 July 2024 | **Nantes - France**

Volume 8

Special Sessions

ISBN: 978-2-912985-01-9
DOI: 10.60691/yj56-np80